JOURNAL OF MATERIALS SCIENCE **38** (2003) 843–852

Crystallization study of (TiO_2, ZrO_2)-rich SiO_2-Al_2O_3-CaO glasses

Part I *Preparation and characterization of zirconolite-based glass-ceramics*

P. LOISEAU, D. CAURANT*, O. MAJERUS, N. BAFFIER
Laboratoire de Chimie Appliquée de l'Etat Solide (UMR CNRS 7574), ENSCP, 11 rue Pierre et Marie Curie, 75231 Paris, France
E-mail: caurant@ext.jussieu.fr

C. FILLET
Commissariat à l'Énergie Atomique (CEA), Direction de l'Energie Nucléaire Centre de la Vallée du Rhône, DIEC/SCDV/LEBM, 30207 Bagnols sur Ceze, France

Nuclear power reactors generate long-lived radionuclides such as minor actinides (Np, Am, Cm) which are mainly responsible for the long term radiotoxicity of high level nuclear wastes obtained after reprocessing of nuclear spent fuel. Specific highly durable matrices such as glass-ceramics appear as good candidates for the immobilization of minor actinides. This work concerns the synthesis and the characterization of zirconolite ($CaZrTi_2O_7$) based glass-ceramics prepared by controlled devitrification of (TiO_2, ZrO_2)-rich SiO_2-Al_2O_3-CaO parent glasses for which neodymium was selected to simulate the radioactive trivalent minor actinides. The present study reports the effect of increasing TiO_2, ZrO_2 and CaO amounts in glass composition on the structure and the composition of the zirconolite crystals (formed as the only crystalline phase in the bulk of the glass), on their nucleation rate I(Z) and on the volume proportion of crystalline phase V of the glass-ceramics. It appears that I(Z) and V strongly increase when the parent glass composition changes. Neodymium electron spin resonance (ESR) shows that the total amount of Nd^{3+} ions incorporated in the zirconolite phase increases with TiO_2, ZrO_2 and CaO amounts in parent glass composition.

1. Introduction

High level radioactive wastes (HLW), produced either by the reprocessing of nuclear spent fuel or by the military activity, contain fission products and minor actinides (Np, Am and Cm) which must be efficiently isolated from biosphere. All these radionuclides together with inactive fission products are currently immobilized, without separation, in aluminoborosilicate glassy matrices prepared in nuclear vitrification plants [1]. However, in recent years, there has been a considerable interest in the development of more durable specific matrices designed for the specific immobilization of long-lived radionuclides such as actinides (α-emitters) which are mainly responsible for HLW long term radiotoxicity and which could originate either from an enhanced reprocessing of nuclear spent fuel (minor actinides) or from excess weapons plutonium wastes [2]. Such wasteforms must incorporate high actinide amounts and must exhibit particularly good long term behavior (high chemical durability and self radiation resistance).

Zirconolite (nominally $CaZrTi_2O_7$) is a crystalline phase well-known for its capacity to incorporate high actinide and lanthanide amounts as solid solution in the calcium and zirconium sites of its crystal lattice [3–5]. Moreover this phase shows a very good long-term behavior in spite of its amorphization tendency under α-decay (low effect of radiation damage on its very good chemical durability) [6–9]. However, preparation of pure zirconolite, via ceramic route by classical hot pressing techniques for instance, is relatively difficult to adapt to nuclear industry. Indeed, this kind of process, unlike well-established radioactive glass melting, requires several steps and is discontinuous. So, it is mainly suited for the preparation of small samples. Moreover, phases with uncontrolled chemical durability can form at grain boundaries.

To benefit at the same time from the ease of glass preparation and from the very good long term behavior of ceramics in comparison with borosilicate nuclear glasses, the preparation of glass-ceramic wasteforms

*Author to whom all correspondence should be addressed.

consisting of small zirconolite crystals (which would preferentially incorporate actinides) homogeneously dispersed in a highly durable glassy matrix—acting as a second barrier of containment—may be considered as an interesting alternative. In this case, the matrices could be prepared by classical glass technology followed by a controlled crystallization stage either by reheating the glass or by slowly cooling the melt [10].

Previous studies showed that controlled devitrification of a particular glass composition (referred as glass A in this paper) belonging to the SiO_2-Al_2O_3-CaO-TiO_2-ZrO_2-Na_2O-Nd_2O_3 system (with $0 \leq Nd_2O_3 \leq 10$ wt% (2.2 mol.%)) led to zirconolite as the only crystalline phase in the bulk (internal crystallization) for isothermal crystal growth thermal treatments performed at T_c ranging from 1000° to 1200°C [11–14]. In these studies, trivalent minor actinides (Am^{3+}, Cm^{3+}) were simulated by neodymium ions (Nd^{3+}) because of their similar radii [15] and because lanthanides (4f elements) are usually considered as good minor actinides (5f elements) surrogates [16]. Aqueous alteration tests indicated that these wasteforms exhibited very low leaching rate [8]. For $T_c < 1000$°C, a phase with a defect-fluorite structure corresponding to a highly disordered zirconolite is observed in the bulk [13]. For $T_c \geq 1250$°C, baddeleyite (m-ZrO_2) crystals form in the bulk at the expense of zirconolite [12]. The liquidus temperature of the melt is near 1400°C. However, different crystallization processes and different crystalline phases occur on glass surface: a thin crystallized layer—consisting essentially of elongated titanite (nominally $CaTiSiO_5$) and anorthite (nominally $CaAl_2Si_2O_8$) crystals—forms after heterogeneous nucleation (surface crystallization). Nd^{3+} ions were showed to enter preferentially in the calcium site of zirconolite crystals formed in the bulk and in the calcium site of titanite crystals grown near sample surface whereas anorthite crystals did not incorporate neodymium [17]. The existence of this thin crystallized layer near sample surface is not very serious because titanite is a crystalline phase known for its capacity to incorporate actinides, and titanite-based glass-ceramics have already been proposed for HLW immobilization [3, 18, 19]. The volume fraction V of zirconolite crystals formed in the bulk of the glass-ceramics was evaluated using energy dispersive X-ray analysis (EDX) and density measurements: V ($T_c = 1200$°C) ≈ 9% and V ($T_c = 1050$°C) ≈14% [20]. These percentages of crystalline phase are low in comparison with commercial glass-ceramics for which V is often higher than 90% [21]. This result is not surprising because the parent glass contains small TiO_2 and ZrO_2 concentrations and the composition of the phase crystallizing in the bulk (zirconolite) is fairly different to the one of the parent glass. Moreover, SiO_2 is not known to enter in the $CaZrTi_2O_7$ structure (lack of tetrahedral sites) [22]. In spite of this low volume fraction of crystalline phase, electron spin resonance (ESR) results showed that approximately 36% of the total amount of the Nd^{3+} ions initially present in the parent glass could be incorporated in the zirconolite phase for a 6 wt% Nd_2O_3 glass composition devitrified at $T_c =$ 1050°C [17].

In order to increase at the same time the proportion of crystalline material in the bulk of the glass-ceramics and the amount of neodymium incorporated in the zirconolite phase, two new glasses (referred as glasses B and C in this paper) were prepared and their crystallization behavior was studied. For these two compositions, the CaO, ZrO_2 and TiO_2 amounts were increased in comparison with glass A. These three oxides—which are necessary for zirconolite crystallization—were increased according to zirconolite stoichiometry (1:1:2). In this paper (Part 1), the devitrification behavior of the three glass compositions (A, B and C) was compared using isothermal treatments and the glass-ceramics obtained were studied by XRD, scanning electron microscopy (SEM) and ESR. In part 2 of this work [23], crystallization of the three glass compositions was followed by differential thermal analysis (DTA) in order to investigate nucleation mechanisms and to extract crystal growth activation energies for the phases that form either in the bulk or on glass surface.

2. Experimental

2.1. Glass compositions and preparation

The three glass compositions prepared for this study are reported in Table I:

– As indicated in the Introduction, glass A corresponds to a basic composition for which zirconolite is the only crystalline phase to nucleate in the bulk [11–14]. This glass can be considered as a (TiO_2, ZrO_2)-rich SiO_2-Al_2O_3-CaO glass in which TiO_2 and ZrO_2 were introduced with a molar ratio [Ti]/[Zr] close to 2.2 [11]. It can be noticed that this last value is

TABLE I Composition (in oxide weight and molar percentage) and glass transformation temperature (onset of DTA endothermic effect) of glasses A, B and C

	SiO_2	Al_2O_3	CaO	TiO_2	ZrO_2	Nd_2O_3	Na_2O	T_g (°C)
Glass A								
Weight%	40.57	11.95	19.63	12.45	8.46	6.00	0.94	762 ± 2
Mol%	48.23	8.37	25.01	11.14	4.90	1.27	1.08	
Glass B								
Weight%	36.07	10.62	19.18	15.98	11.31	6.00	0.84	760 ± 2
Mol%	43.83	7.61	24.97	14.61	6.70	1.30	0.98	
Glass C								
Weight%	32.47	9.56	18.82	18.81	13.59	6.00	0.75	760 ± 2
Mol%	40.17	6.97	24.94	17.50	8.20	1.32	0.90	

only slightly higher than the molar ratio of stoichiometric zirconolite ([Ti]/[Zr] = 2). The simplified calcium aluminosilicate composition is located near the silica-rich eutectic point of the corresponding ternary phase diagram [24]. Glasses belonging to this system are known to be easy to melt (low liquidus temperature near the eutectic point: 1170°C), and to exhibit a good chemical durability (lack of alkali ions) and a low bulk crystallization tendency [10, 25]. Thus, such glasses hardly lead to the formation of silicate crystals by internal nucleation. This property is very interesting in our case in order to avoid the internal crystallization of undesirable crystalline phases at the expense of zirconolite. Moreover it was showed that zirconolite crystals which form in the bulk of glass A do not act as efficient nucleating agent for silicate phases [12, 13]. 6 wt% Nd_2O_3 were used to simulate radioactive minor actinides. This weight percentage was kept constant for the three glasses and is equivalent to 9.2 wt% Am_2O_3 on a molar basis. A small amount of Na_2O (≈1 wt%) was also added to the glass compositions in order to perform chemical durability tests which are not presented here. Indeed, Na^+ ion can be considered as a good chemical alteration tracer of the residual glass (which is less durable than zirconolite) since it is not incorporated into zirconolite crystals and is not retained in alteration gels [26].

– For glasses B and C, the relative molar ratios of SiO_2, Al_2O_3 and Na_2O are the same as for glass A. But in order to increase the amount of crystalline phase in the bulk of glass-ceramics, the amounts of CaO, ZrO_2 and TiO_2 (the three oxides constituting zirconolite) in glass composition were increased. Composition changes were made as followed: for 100 moles of glass A, 2.5 and 5 moles of ZrO_2 were added respectively (Table I) for glasses B and C. This corresponds to a ZrO_2 enrichment of approximately 50 and 100 mol% respectively. At the same time, the CaO and TiO_2 amounts were increased according to zirconolite stoichiometry in comparison with silica, alumina and soda.

Glasses were prepared from reagent-grade SiO_2, Al_2O_3, $CaCO_3$, TiO_2, ZrO_2, Na_2CO_3 and Nd_2O_3. For each composition a 50 g batch was melted and refined at 1550°C for 10 h in a platinum crucible using an electric furnace. Melts were poured in water, ground in an agate mortar, sieved at 800 μm and remelted for 4 h at 1550°C (1650°C for glass C) to ensure homogeneity. Melts were then cast to room temperature in metallic moulds to form small glass cylinders (14 mm diameter and 10 mm high). Samples for isothermal devitrification study were annealed at 775°C for 2 h (glass transformation temperature onset $T_g \approx 760$°C, see Table I) and slowly cooled to room temperature in order to relieve internal stresses before cutting. DTA experiments were performed on unannealed glass samples [23].

Glass A was obtained without problems, whereas a ZrO_2-rich deposit consisting of large baddeleyite crystals (about 10 μm in diameter) with a few small zirconolite crystals was observed on the bottom of platinum crucibles for glasses B and C after the first melting stage. This crystalline layer disappeared and transparent samples were obtained after grinding and remelting the samples at respectively 1550° and 1650°C for glasses B and C. Study of the deposit by energy dispersive X-ray analysis (EDX) indicated that the ZrO_2 (baddeleyite) grains contained significant amounts of TiO_2 (ZrO_2 is known for its ability to incorporate TiO_2 in its structure [27]). This result shows that these crystals do not originate from unmelted ZrO_2 grains of the batch but have probably crystallized from the melt. The existence of this deposit can be explained by the lack of stirring during batch melting and by the increase of the liquidus temperature for compositions B and C.

2.2. Glass-ceramics preparation and characterization

Devitrification of the three glasses was performed by controlled crystallization heat treatments. After annealing, all the samples were firstly nucleated at $T_N = 810$°C for 2 h. This value is slightly higher than T_g (≈760°C) and than the temperature $T_{max} = 790$°C corresponding to the maximum of zirconolite nucleation rate in glass A [20]. After nucleation, the samples were immediately transferred in a furnace preheated at $T_c = 1050$° or 1200°C for crystal growth for 2 h. The glass-ceramics were then directly annealed at 775°C for 2 h. After slow cooling they were cut in order to isolate the bulk of the sample from the surface. For glass C, a crystal growth thermal treatment at $T_c = 860$°C for 2 h was also performed to prepare a glass-ceramic with zirconolite crystals having the defect-fluorite structure.

Glasses and crystallized samples were characterized with the help of various techniques. Powder X-ray diffraction (XRD) patterns were recorded using a Siemens D5000 instrument with Co K_α radiation ($\lambda = 1.78897$ Å). SEM and EDX analysis were performed at 15 kV on polished and carbon coated samples with a Hitachi S2500 microscope equipped with a PGT EDX analyzer. An ESR spectrometer Bruker ESP 300e operating at X-band ($\nu \approx 9.5$ GHz) and equipped with a TE102 rectangular cavity and an Oxford variable temperature accessory was used to follow the incorporation and to estimate the amount of paramagnetic Nd^{3+} ions ($4f^3$) in zirconolite crystals [17].

3. Results and discussion

3.1. XRD and SEM study

As cast and nucleated samples are fully transparent and X-ray amorphous (see Fig. 1a for glass A). EDX analysis results reported in Table II show that there is a relatively good accordance between glass and batch compositions (Table I). This is not surprising because no volatile element is present in glass compositions. After thermal treatment at $T_c = 1050$° or 1200°C and cutting, all the samples are totally opaque and a crystallized layer near the surface is observed. The thickness of this layer ranges from 100–200 μm at $T_c = 1050$°C to 800–2000 μm at $T_c = 1200$°C.

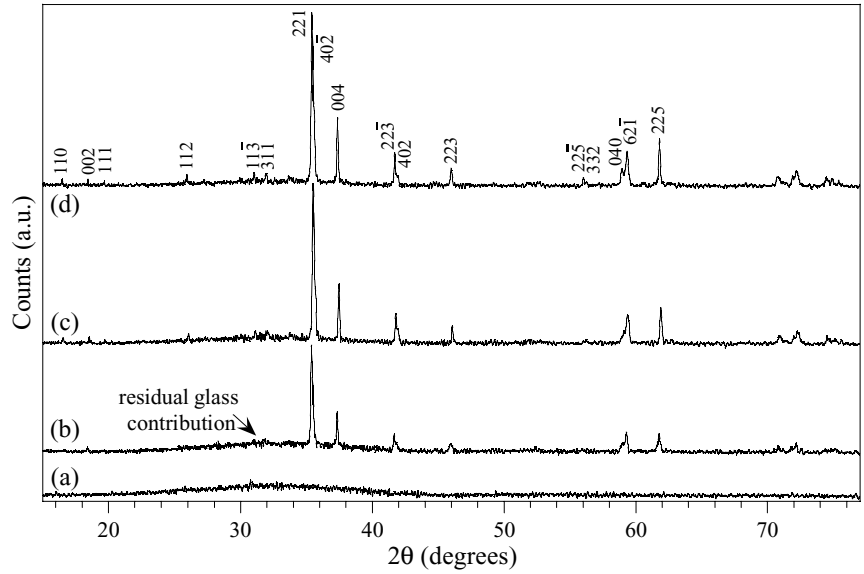

Figure 1 XRD patterns (λCo K_α) of: glass A before (a) and after crystallization (bulk) for 2 h at $T_c = 1200°C$ (b), glasses B and C after crystallization (bulk) for 2 h at $T_c = 1200°C$ (c and d respectively). All the XRD lines are associated with zirconolite-2M crystals formed in the bulk of glass-ceramics.

3.1.1. Crystallization in the bulk of the glass

The XRD patterns recorded for the bulk of glass-ceramics A, B and C (Fig. 1b–d) show that zirconolite is the only crystalline phase to form irrespective of the composition of the parent glass. It is interesting to notice that the following phases: $Ca_2Zr_5Ti_2O_{16}$ (calzirtite), $ZrTiO_4$, $CaTiO_3$ and $CaZrO_3$ (perovskite) reported by Rossell [28] for the CaO-ZrO_2-TiO_2 system, are not detected in our glass-ceramics. Moreover neither ZrO_2 (which is however the first phase to crystallize from the melt as showed in Part 2 of this work [23]) nor $ZrSiO_4$ (zircon) crystals are observed for the two T_c values in spite of the high SiO_2 content in parent glasses (Table I). XRD patterns of the bulk of the three glass-ceramics can be all indexed in the zirconolite-2M monoclinic system (Fig. 1b–d). The zirconolite lattice parameters thus determined are very similar for the three samples (Table III). Crystals composition deduced from EDX analysis (Table II) for the samples prepared at $T_c = 1200°C$ are also almost identical (Table III). It must be noticed that the low amount of silica detected by EDX (Table II) for zirconolite crystals is the result of a small contribution of the residual glass to EDX spectra. The compositions given in Table III were calculated by subtracting the residual glass contribution. Table II also indicates that for the three samples, the composition of the residual glass in the bulk is strongly depleted in TiO_2 and ZrO_2 whereas a SiO_2 and Al_2O_3 enrichment is observed. Moreover, Table III shows that zirconolite lattice parameters depend on T_c. Such an evolution has already been observed in reference [12] for glass A: from XRD patterns simulation and from high resolution transmission electron microscopy observations, this evolution was

TABLE II Compositions determined by EDX analysis for the crystalline phases formed in the bulk (zirconolite) and near the surface (titanite, anorthite) of glasses A, B and C for $T_c = 1200°C$

	SiO_2	Al_2O_3	CaO	TiO_2	ZrO_2	Nd_2O_3	Na_2O
Glass A (wt%)							
Parent glass*	40.57	11.95	19.63	12.45	8.46	6.00	0.94
Residual glass (bulk)	46.59	13.38	20.26	8.53	4.22	5.84	1.14
Zirconolite (bulk)	4.70	3.46	13.55	36.38	32.94	8.50	0.43
Titanite (surface)	27.33	2.56	22.94	25.65	13.09	8.08	0.31
Anorthite (surface)	49.62	32.16	15.62	0.30	0.07	0.07	2.14
Glass B (wt%)							
Parent glass	36.51	10.76	19.20	15.92	10.36	6.58	0.65
Residual glass (bulk)	44.79	12.35	20.76	10.62	4.81	6.02	0.63
Zirconolite (bulk)	1.38	2.20	13.63	40.67	33.76	8.13	0.23
Titanite (surface)	23.61	2.49	22.19	28.43	14.15	8.74	0.37
Anorthite (surface)	49.79	30.04	16.75	1.14	0.38	0.17	1.71
Glass C (wt%)							
Parent glass	32.31	9.14	18.75	18.71	13.63	6.67	0.76
Residual glass (bulk)	42.71	11.85	21.07	12.01	5.32	6.39	0.62
Zirconolite (bulk)	1.46	2.16	13.65	41.68	32.78	7.98	0.27
Titanite (surface)	25.41	2.34	23.24	27.75	12.48	8.41	0.35
Anorthite (surface)	49.72	31.95	15.78	0.33	0.09	0.00	2.13

Composition of the parent glass and of the residual glass remaining between zirconolite crystals in the bulk are also given for the three samples (*: glass A was used as reference sample for EDX analysis).

TABLE III Composition of the zirconolite crystals formed in the bulk of the glass-ceramics A, B and C ($T_c = 1200°C$) determined by EDX analysis

	Zirconolite composition (bulk, $T_c = 1200°C$)					
	Sample A: $Ca_{0.82}Nd_{0.19}Zr_{1.05}Ti_{1.77}Al_{0.17}O_7$		Sample B: $Ca_{0.85}Nd_{0.17}Zr_{1.00}Ti_{1.85}Al_{0.13}O_7$		Sample C: $Ca_{0.84}Nd_{0.17}Zr_{0.97}Ti_{1.89}Al_{0.13}O_7$	
	$T_c = 1050°C$	$T_c = 1200°C$	$T_c = 1050°C$	$T_c = 1200°C$	$T_c = 1050°C$	$T_c = 1200°C$
a (Å)	12.564(2)	12.512(2)	12.560(3)	12.511(4)	12.562(1)	12.498(3)
b (Å)	7.259(1)	7.267(1)	7.255(1)	7.267(2)	7.246(1)	7.267(1)
c (Å)	11.356(2)	11.373(2)	11.354(2)	11.366(2)	11.349(2)	11.367(2)
β (degrees)	100.63(1)	100.63(2)	100.62(2)	100.62(2)	100.62(1)	100.66(2)
Vol (Å^3)	1018(3)	1016(4)	1017(4)	1016(4)	1015(3)	1015(4)

The zirconolite lattice parameters (a, b, c, β) and cell volume (Vol.) obtained by XRD for the three glass-ceramics samples prepared at $T_c = 1050°C$ and $T_c = 1200°C$ are also given. Numbers in parentheses are esd's and apply to the last quoted place.

explained by an increase of the cation ordering in Ca/Zr planes with crystal growth temperature T_c. Moreover, the composition changes from glass A to C do not modify significantly neither the nature nor the structure and the composition of the crystals (zirconolite) growing in the bulk of the glasses (Table III). SEM micrographs showed in Fig. 2 clearly indicate a progressive increase of the volume fraction of zirconolite crystals of glass-ceramics when ZrO_2, TiO_2 and CaO concentrations are raised. SEM images analysis indicates that the amount of crystalline phase is approximately 9, 14 and 19 vol% respectively for the glass-ceramics A, B and C prepared at $T_c = 1200°C$. This result was confirmed by a monotonous increase of the integrated intensity of the zirconolite XRD lines (Figs 1 and 3). Zirconolite particles formed at $T_c = 1050°C$ in glass A exhibit a dendritic microstructure (Fig. 2a). This microstructure becomes hard to observe for glasses B and C (Fig. 2b and c). For these two samples, the size of the zirconolite particles decreases (≈100 nm) and their number strongly increases (Fig. 2b and c). A similar evolution between the three compositions is observed for the glasses heat-treated at $T_c = 1200°C$ (Fig. 2d and f).

Important microstructural changes are clearly observed for glass A between $T_c = 1050°$ and 1200°C. For the highest temperature, the dendritic morphology disappears and elongated zirconolite crystals grow in the bulk. In fact, previous studies showed that this microstructural change was progressive between 1050° and 1200°C and could be due to the decrease of the supercooled liquid viscosity with temperature and to diffusion controlled growth processes (the composition of zirconolite is very different from the one of parent glasses) [12]. Similar microstructural evolutions with temperature were reported in literature for other glass systems for which the crystallization process was incongruent [29–31].

Analysis of Fig. 2 clearly indicates that when the parent glass composition changes from A to C, the number of nuclei strongly increases. Consequently, the

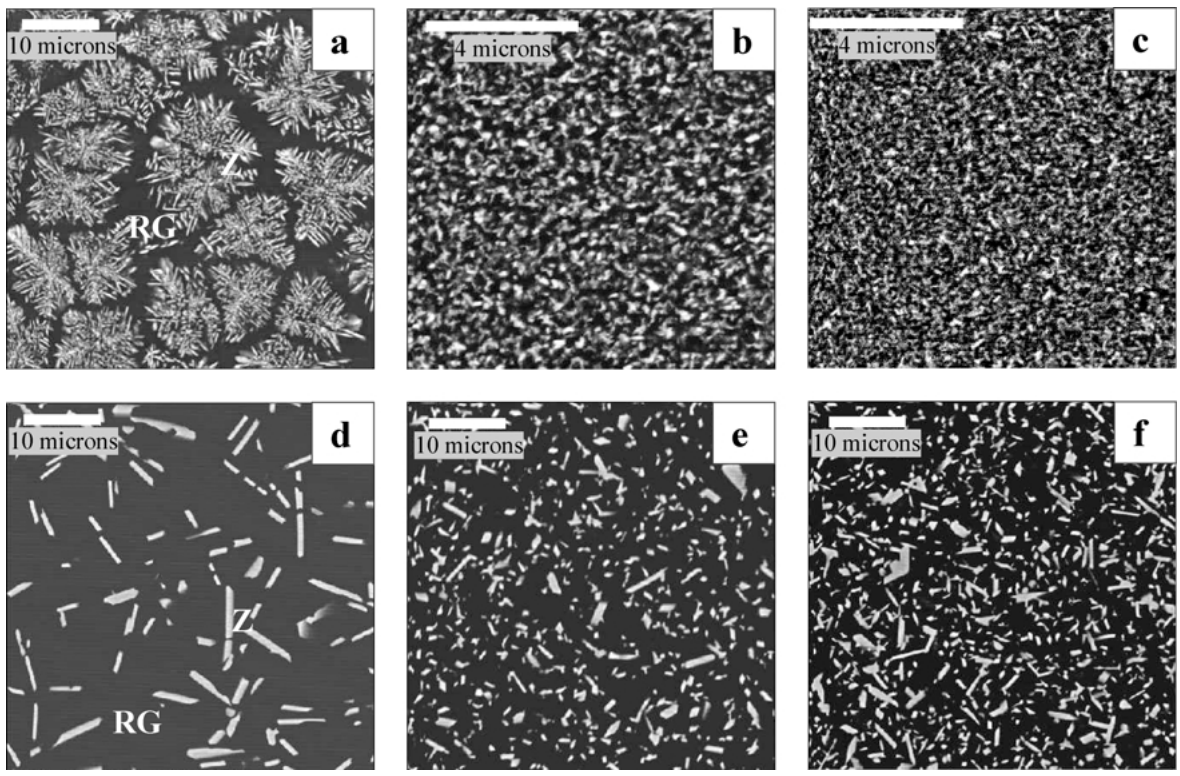

Figure 2 Back-scattered SEM micrographs of the bulk of the glass-ceramics prepared after nucleation for 2 h at $T_N = 810°C$ and crystallization for 2 h at $T_c = 1050°C$ (a, b, c respectively for annealed glasses A, B, C) or $T_c = 1200°C$ (d, e, f respectively for annealed glasses A, B, C). Due to a high concentration of the heaviest elements in zirconolite, the contrast is strong between crystals (white, Z) and residual glass (black, RG).

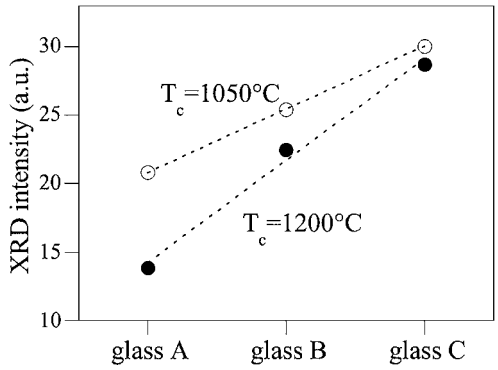

Figure 3 Evolution of XRD pattern intensity of the bulk of the glass-ceramics A, B and C for $T_c = 1050°C$ and $T_c = 1200°C$. Intensity values (in arbitrary unit) were obtained by integration of the lines of XRD patterns of Fig. 1 which were recorded in the same conditions (size fraction, amount of powder, apparatus parameters).

corresponding zirconolite nucleation rates in bulk for the three glasses can be ranked in the following order: I_{bulk} (A) $\ll I_{bulk}$ (B) $<$ I_{bulk} (C). This evolution can be explained by an increase of the zirconolite crystallization driving force (corresponding to the free energy difference $|\Delta G_c|$ between the partially crystallized glass-ceramic and the supercooled melt) due to ZrO_2, TiO_2 and CaO enrichment in the parent glass. Such glass composition changes towards the composition of the crystallizing phase are well known to raise $|\Delta G_c|$ [32]. The nucleation rate evolution observed could be also explained by a decrease of the nuclei-liquid interfacial energy σ and/or of the nucleation kinetic barrier (decrease of the activation energy associated with short-range diffusion near the surface of nuclei) [32].

TiO_2 and ZrO_2 are oxides classically added to glass-ceramics parent glass compositions because of their tendency to induce glass-in-glass separation and/or to form small crystals on which the main crystalline silicate phases may nucleate heterogeneously [33, 34]. High resolution transmission electron microscopy (HRTEM) studies were performed on glass A submitted to a very long nucleation stage at 810°C (10 days). No indication of amorphous glass separation was observed before and after nucleation. Nevertheless, small crystals of 300–400 nm in diameter having a defect-fluorite structure were observed [20]. Thus, it seems reasonable to assume that zirconolite (in fact its defect-fluorite form observed for $T_c < 1000°C$) nucleates homogeneously in glass bulk, but the heterogeneous nucleation of zirconolite on ZrO_2 nuclei cannot be totally excluded [23]. It is interesting to notice that for the three compositions studied, zirconolite crystals never act as nucleating agent for silica rich crystalline phases such as titanite and anorthite. On the contrary, these phases nucleate heterogeneously on sample surface. This is probably due to an epitaxial discordance between zirconolite and the silicate crystalline phases [10, 35].

As indicated in the Introduction, for $T_c < 1000°C$ a defect-fluorite phase forms in the bulk of glass A. This phase transforms irreversibly into zirconolite–2M for $T_c \geq 1000°C$ [13]. These results were confirmed by the DTA study of glasses B and C [23]: defect-fluorite crys-

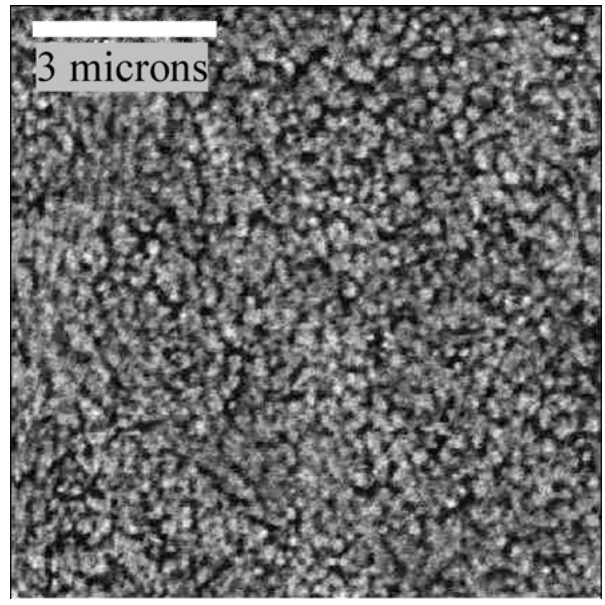

Figure 4 Back-scattered SEM micrograph of glass C after thermal treatment for 2 h at $T_c = 860°C$ showing a very high density of crystals with defect-fluorite structure.

tals firstly nucleate and grow in the bulk and transform into zirconolite at higher temperature. Similar crystallization scenario and phase transformation were observed by Vance *et al.* [36] by heating a zirconolite amorphous alkoxide precursor. Isothermal treatment of glass C during 2 h at $T_c = 860°C$ leads only to the formation of crystals having a defect-fluorite structure (860°C is only slightly lower than the corresponding DTA exothermic peak, see Part 2 of this work [23]). The corresponding XRD pattern and SEM image are showed respectively in Figs 4 and 5. A very high density of defect-fluorite crystals forms in the bulk (Fig. 4) whereas titanite and anorthite crystals are not observed on glass surface at this temperature (lack of silicate crystallized layer). The XRD pattern (Fig. 5) can be indexed in the cubic system with $a = 5.041$ Å. This value is very similar to the one obtained for the defect-fluorite phase formed in glass A at 950°C ($a = 5.045$ Å) and to the one reported by Vance *et al.* [36] for their intermediate defect-fluorite phase ($a = 5.01$ Å).

All these results indicate that the composition changes between glass A and glass C do not modify the

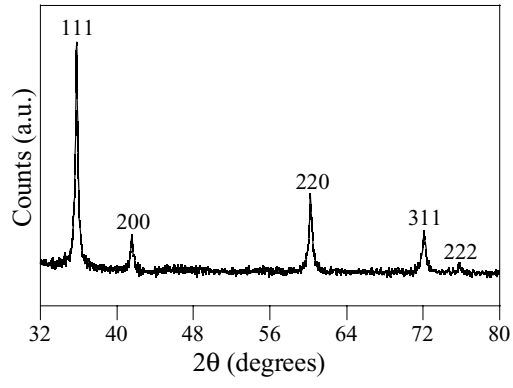

Figure 5 XRD pattern (λCo K_α) of glass C (bulk) after crystallization for 2 h at 860°C. All the XRD lines are associated with the cubic defect-fluorite structure.

crystallization and the phase transformation processes occurring in the bulk of the glass but induce a strong increase of the zirconolite nucleation rate and of the percentage of crystalline material of glass-ceramics.

3.1.2. Crystallization from glass surface

SEM images of the crystallized layers formed on glasses A, B and C for $T_c = 1050°C$ are showed in Fig. 6. For the three compositions, the same crystalline phases are observed: titanite and anorthite elongated crystals have grown towards the bulk after heterogeneous nucleation on glass surface. XRD patterns recorded for the crystallized surface layer (Fig. 7), confirmed these results (formation of titanite and anorthite) and indicate that the amount of residual glass is lower in this layer than in the bulk of glass-ceramics. Contrarily to anorthite crystals which show a needlelike morphology, titanite crystals exhibit small dendritic branches almost perpendicular to their main crystal growth direction for $T_c = 1050°C$. These differences are not easy to explain but may be due to differences of crystal structures and of crystal growth processes for titanite and anorthite. For $T_c = 1200°C$, an increasing quantity of small zirconolite and baddeleyite crystals containing titanium is also observed among the silicate crystals when composition changes from A to C. Fig. 8 shows a SEM image of the crystals formed near the surface of glass B at $T_c = 1200°C$. The small quantity of

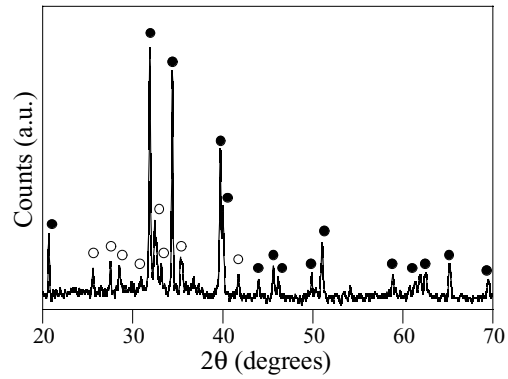

Figure 7 XRD pattern (λCo K_α) of the crystallized surface layer formed on glass A after thermal treatment for 2 h at $T_c = 1200°C$. (○: anorthite, ●: titanite).

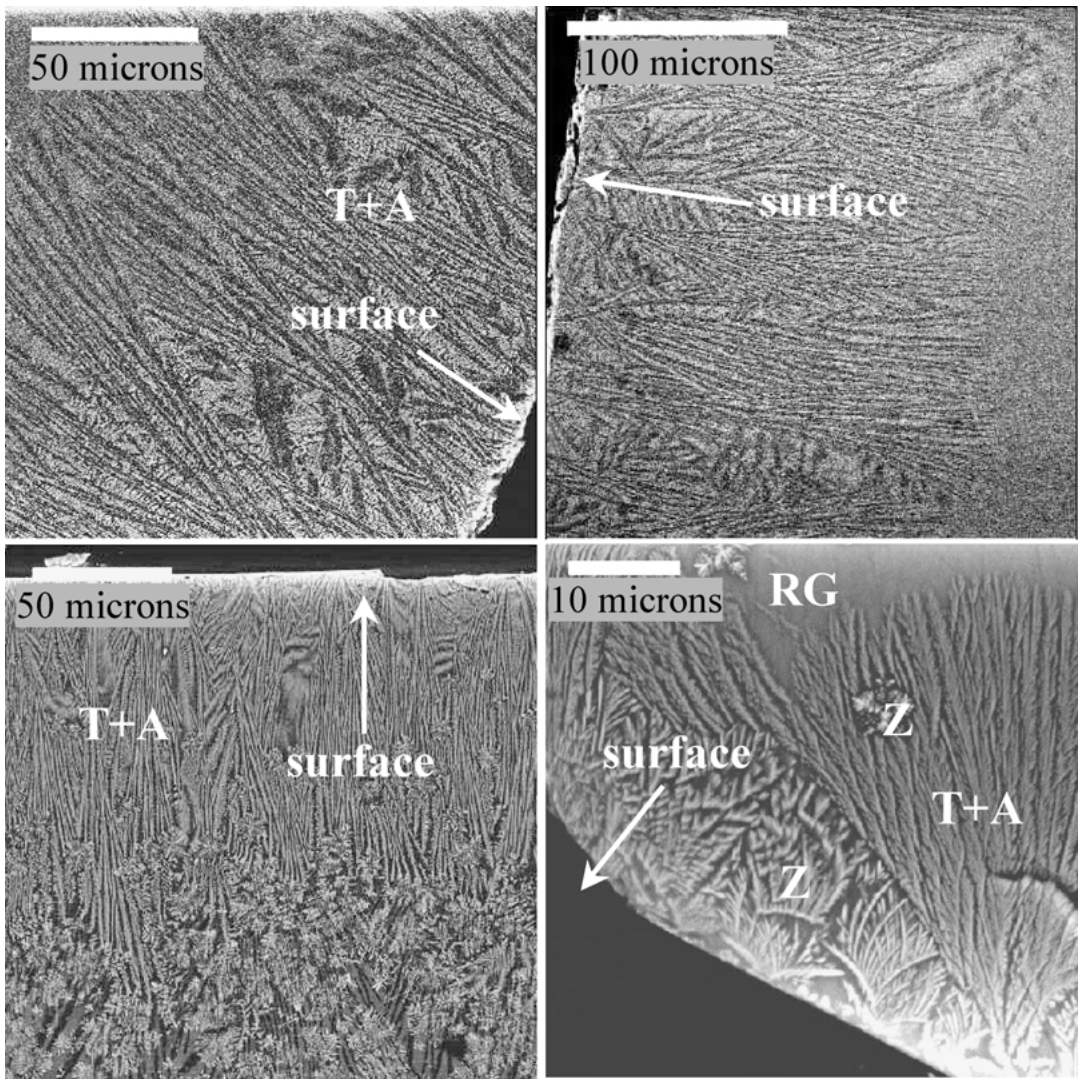

Figure 6 Back-scattered SEM images of the crystallized layer formed on glass A (bottom left), B (upper left) and C (upper right) surface after heating for 2 h at $T_c = 1050°C$. Titanite appears as white crystals whereas anorthite (which contained the lightest elements of the parent glass, see Table II) are darker than residual glass. The very thin crystallized layer observed on the surface of glass A after nucleation for 2 h at $T_N = 785°C$ and crystallization for 10 min at $T_c = 1050°C$ is showed in (bottom right). (Z: zirconolite, T: titanite, A: anorthite, RG: residual glass).

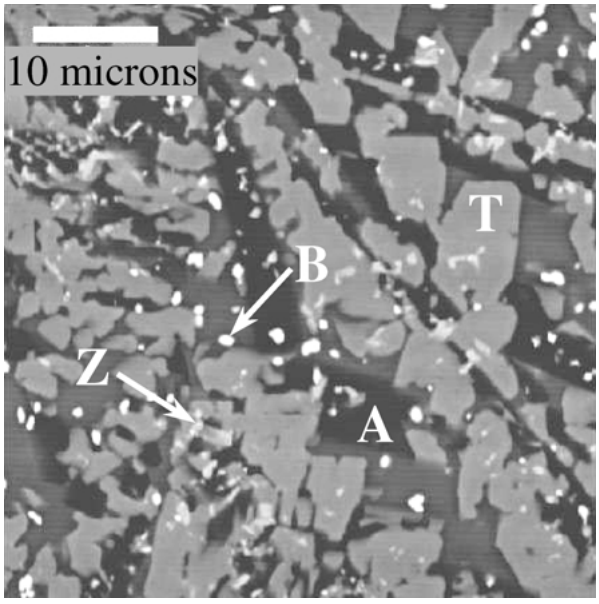

Figure 8 Back-scattered SEM images of the crystallized layer formed on glass B after heating for 2 h at $T_c = 1200°C$. (T: titanite (gray), A: anorthite (black), B: baddeleyite (white), Z: zirconolite (light gray)).

zirconolite crystals observed in this figure indicates that these crystals, that were formed near glass surface before the progression of silicate crystalline phases (titanite and anorthite), were then embedded by the silicate crystals growing from the surface: the growing of these latter phases, and particularly of titanite, leads to a partial dissolution of zirconolite crystals. Whereas the crystallized layer thickness l does not significantly change between the different samples for $T_c = 1050°C$ ($l \approx 150$–$200\ \mu m$), an increasing evolution of l is observed for $T_c = 1200°C$ (l(glass A) ≈ 800–$900\ \mu m$, l(glass B) $\approx 1000\ \mu m$, l(glass C) $\approx 2000\ \mu m$). This evolution of l with glass composition for $T_c = 1200°C$ can be explained by a decrease of the thermodynamic and kinetic barriers corresponding to the crystal growth of titanite for the highly TiO_2 concentrated samples. For $T_c = 1050°C$, the dendritic zirconolite crystals which form in glass bulk near glass surface, probably disturb titanite and anorthite crystal growth. Besides, short thermal treatments ($t \approx 10$ min) carried out at $T_c = 1050°C$ indicate that zirconolite crystals can also nucleate heterogeneously on glass surface (Fig. 6). Therefore, an increasing amount of ZrO_2 and TiO_2 in the parent glass may also disturb titanite and anorthite nucleation rate by decreasing the number of available surface sites for heterogeneous nucleation due to a greater competition with zirconolite. This observation may explain the shift towards higher temperature of the exothermic DTA peaks due to anorthite and titanite crystallization between the three samples [23]. It is interesting to notice that complementary studies performed on glass A with only a very small number of nuclei showed that the crystal growth rate of titanite u_T and anorthite u_A are higher than the one of zirconolite u_Z for T_c ranging from 1000°C to 1200°C [20]: $u_T \approx u_A > u_Z$. This information is difficult to extract from the study of SEM images for the highly nucleated samples because of the impingement of the crystals (Figs 2 and 6). The higher growth rate of silicate phases originates essentially from kinetic reasons. For zirconolite, SiO_2 is totally rejected in the residual glass from the growing crystal front. This is not the case for anorthite and titanite because silica is one of the main oxides of their composition. Consequently diffusional and reconstructive phenomena which occur in crystal growth, are more slowed down for zirconolite.

It can be noticed that the strong tendency of titanite to nucleate heterogeneously was also observed by Hayward [18, 19] either on glass surface or on boundaries between separated glassy phases for compositions belonging to the system Na_2O-Al_2O_3-CaO-TiO_2-SiO_2.

3.2. Neodymium incorporation in zirconolite crystals

EDX results obtained for $T_c = 1200°C$ (Table II) show a strong enrichment of neodymium in the zirconolite phase for all the samples. However, the composition of the bulk residual glass indicates only a weak neodymium concentration depletion in comparison with the corresponding parent glass. The formula of zirconolite crystals formed in the three glasses is reported in Table III. It shows that Nd^{3+} ions substitute preferentially for Ca^{2+} ions with a charge compensation mainly ensured by Al^{3+} ions in titanium sites following the general formula: $Ca_{1-x}Nd_xZrTi_{2-x}Al_xO_7$. For the compositions studied here, between $x = 0.17$ and 0.19 formula units of neodymium ions are substituted for calcium ions. This shows that the composition changes between the three glasses do not significantly modify neodymium incorporation in zirconolite crystals. However, because of the increase of the proportion of crystalline phase, the total amount of Nd^{3+} ions incorporated in the crystalline phase increases from glass-ceramics A to C. In order to estimate the ratio R corresponding to the amount of neodymium incorporated in zirconolite to the total amount of neodymium in glass-ceramics, ESR spectra were recorded for the bulk of the three samples for $T_c = 1050°$ and 1200°C. Spectra corresponding to glasses A and C heated at 1200°C are showed in Fig. 9. The contribution of Nd^{3+} ions in zirconolite crystals (Z) and in residual glass (RG) can be separated (see dotted line spectra in Fig. 9) and R can

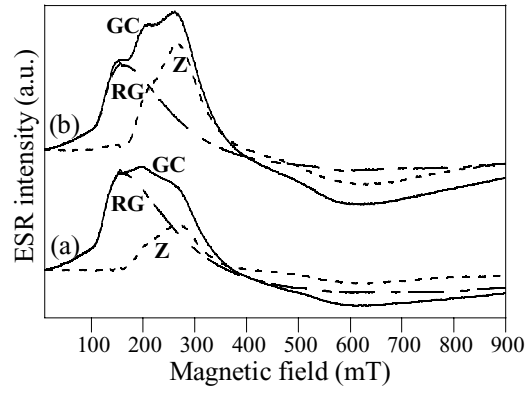

Figure 9 Neodymium X-band ESR spectra recorded at 12 K for the bulk of glass-ceramic A (a) and C (b) prepared at $T_c = 1200°C$ for 2 h (GC spectra). The individual contributions of Nd^{3+} ions located in the zirconolite phase (Z spectra) and in the residual glass (RG spectra) are showed in dotted lines.

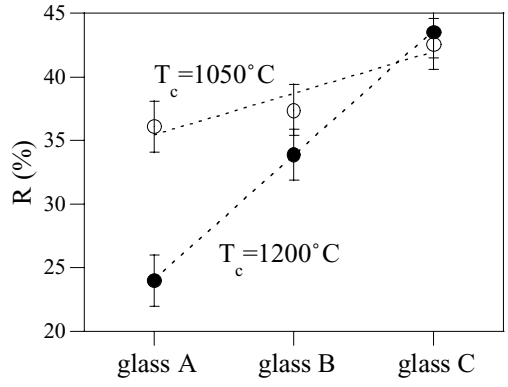

Figure 10 Effect of parent glass composition and crystal growth temperature (T_c) on the percentage R of Nd^{3+} ions incorporated in the zirconolite crystalline phase formed in the bulk of glass-ceramics.

be estimated by double computer integration of ESR signals as described in [17]. A strong increase of the contribution of Nd^{3+} ions in the zirconolite phase is observed between glasses A and C. The R values obtained are reported in Fig. 10. It clearly appears that R increases with the glass-ceramic proportion of zirconolite crystals. This can be understood because the composition of zirconolite crystals remains almost constant whereas V increases from glass A to C. For glass A, the decrease of R for the highest T_c value (Fig. 10) is mainly due to a decrease in volume crystalline material. This can be associated with a higher solubility of zirconolite constituents in the melt when T_c increases [17]. The difference between the R values for the two crystal growth temperatures is smaller for glass B and is negligible for glass C (Fig. 10). A similar evolution with T_c is observed concerning the proportion of crystalline phase for these two compositions (Fig. 3). This indicates that R evolution is mainly due to changes in the total amount of zirconolite between the samples (changing either T_c or glass composition). It is interesting to notice that approximately 43% of Nd^{3+} ions of the glass-ceramic C are incorporated in the zirconolite crystals formed in the bulk of the glass-ceramics (Fig. 10). However, this result can seem a little disappointing as the ideal case would correspond to 100% incorporation of Nd^{3+} ions in zirconolite crystals. Several comments can be made:

- The partitioning of Nd^{3+} ions between zirconolite crystals and the residual glass obey to a thermodynamic equilibrium. Therefore, it cannot seem very realistic to expect a complete incorporation of Nd^{3+} ions in the crystalline phase (this would imply an infinite equilibrium constant).
- As the crystallization of zirconolite in glass-ceramics is incongruent and as its oxide constituents (especially ZrO_2) are relatively little soluble in the parent glass, the amount of crystalline phase which can be formed remains necessarily relatively low. This limitation prevents from reaching very high R values.

Despite these comments, zirconolite-based glass-ceramics keep decisive advantages against other waste-form types such as ceramics. Notably, glass-ceramics can accommodate large fluctuations of the waste composition thanks to the presence of the residual glass. For example, glass-ceramics could tolerate an incomplete separation of actinides from the fission products of HLW, which would be much more doubtful in the case of ceramics.

4. Conclusions

(TiO_2, ZrO_2)-rich calcium aluminosilicate glasses were prepared and their behavior during devitrification (isothermal treatments of nucleation and crystal growth) was studied in order to develop zirconolite ($CaZrTi_2O_7$) based glass-ceramics for minor actinides immobilization. From the experimental results obtained for three parent glass compositions with increasing TiO_2, ZrO_2 and CaO amounts, the following main conclusions can be drawn:

1. For all the compositions studied, zirconolite is the only crystalline phase that forms in the bulk of the glass-ceramics at least for crystal growth temperatures $T_c = 1050°$ and 1200°C. The composition of these crystals and their lattice parameters do not significantly vary between the three glass compositions.
2. When the TiO_2, ZrO_2 and CaO contents in parent glass are raised, a strong increase of the volume fraction of zirconolite in glass-ceramics (from 9 vol% to 19 vol%) and of the zirconolite nucleation rate in the bulk of the glass are observed. This evolution can be explained by an increase of the crystallization driving force with composition changes.
3. The formation of a crystallized surface layer constituted mainly of silicate phases (titanite and anorthite) is observed for all the compositions. These crystals nucleate heterogeneously on glass surface and grow towards the bulk of the glass samples. However, they do not nucleate neither directly in the bulk of the glass (internal nucleation) nor on the surface of zirconolite crystals by heterogeneous nucleation. This clearly shows that zirconolite is not an efficient nucleating agent for titanite and anorthite.
4. 6 wt% Nd_2O_3 were added to all the glass compositions to simulate radioactive trivalent minor actinide oxides. EDX study of the zirconolite crystals grown at $T_c = 1200°$C indicates that approximately 20% of the calcium sites are substituted by Nd^{3+} ions. In this case the charge compensation is mainly ensured by the incorporation of equimolar amounts of Al^{3+} ions in the titanium sites of the zirconolite structure. The evolution of the relative amount R of Nd^{3+} ions incorporated in the zirconolite phase estimated by ESR is essentially due to an increase of the percentage of crystalline phase of the glass-ceramics. The best neodymium incorporation results are obtained for the composition prepared with the highest TiO_2, ZrO_2 and CaO amounts (glass C). In this case, 43% of the Nd^{3+} ions are incorporated in zirconolite crystals. For these ions, the glass-ceramic matrix thus acts as a double containment barrier. Composition changes are currently in progress in order to increase again R. Moreover, better incorporation results are expected for lower Nd_2O_3 concentrations in parent glass [17].

References

1. W. LUTZE, in "Radioactive Waste Forms for the Future," edited by W. Lutze and R. C. Ewing (Elsevier Science Publishers B. V., 1983) p. 3.
2. I. W. DONALD, B. L. METCALFE and R. N. J. TAYLOR, *J. Mater. Sci.* **32** (1997) 5851.
3. E. R. VANCE and D. K. AGRAWAL, *Nuclear and Chemical Waste Management* **3** (1982) 229.
4. P. E. FIELDING and T. J. WHITE, *J. Mater. Res.* **2**(3) (1987) 387.
5. E. R. VANCE, C. J. BALL, R. A. DAY, K. L. SMITH, M. G. BLACKFORD, B. D. BEGG and P. J. ANGEL, *J. Alloys Comp.* **213–214** (1994) 406.
6. W. J. WEBER, R. C. EWING, C. R. A. CATLOW, T. DIAZ DE LA RUBIA, L. W. HOBBS, C. KINOSHITA, HJ. MATZKE, A. T. MOTTA, M. NASTASI, E. K. H. SALJE, E. R. VANCE and S. J. ZINKLE, *J. Mater. Res.* **13** (1998) 1434.
7. C. R. LUMPKIN, R. C. EWING, B. C. CHAKOMAKOS, R. B. GREEGOR, F. W. LYTLE, E. M. FOLTYN, F. W. CLINARD JR., L. A. BOATNER and M. M. ABRAHAM, *ibid.* **1**(4) (1986) 564.
8. T. ADVOCAT, P. J. MCGLINN, C. FILLET, G. LETURCQ, S. SCHULLER and A. BONNETIER, in Scientific Basis for Nuclear Waste Management XXIV, *Mat. Res. Soc. Symp. Proc.* **663** (2001) 277.
9. J. W. WALD and W. J. WEBER, in "Advances in Ceramics," vol. 8: Nuclear Waste Management, edited by G. G. Wicks and W. A. Ross (Am. Ceram. Soc., 1984) p. 71.
10. Z. STRNAD, in "Glass-Ceramic Materials. Glass Science and Technology," vol. 8 (Elsevier, Amsterdam, 1986) p. 114.
11. C. FILLET, J. MARILLET, J. L. DUSSOSSOY, F. PACAUD, N. JACQUET-FRANCILLON and J. PHALIPPOU, *Environmental Issues and Waste Management Technologies in the Ceramic and Nuclear Industries III* **87** (1997) 531.
12. P. LOISEAU, D. CAURANT, N. BAFFIER, L. MAZEROLLES and C. FILLET, in Scientific Basis for Nuclear Waste Management XXIV, *Mat. Res. Soc. Symp. Proc.* **663** (2001) 179.
13. P. LOISEAU, D. CAURANT, N. BAFFIER and C. FILLET, *Verre* **7**(1) (2001) 8.
14. T. ADVOCAT, C. FILLET, J. MARILLET, G. LETURCQ, J. M. BOUBALS and A. BONNETIER, in Scientific Basis for Nuclear Waste Management XXI, *Mat. Res. Soc. Symp. Proc.* (1998) p. 55.
15. R. D. SHANNON, *Acta Cryst.* A **32** (1976) 751.
16. K. B. KRAUSKOPF, *Chem. Geol.* **55** (1986) 323.
17. P. LOISEAU, D. CAURANT, N. BAFFIER and C. FILLET, in Scientific Basis for Nuclear Waste Management XXIV, *Mat. Res. Soc. Symp. Proc.* **663** (2001) 169.
18. P. J. HAYWARD, *Glass Technol.* **29**(4) (1988) 122.
19. *Idem.*, in "Radioactive Waste Forms for the Future," edited by W. Lutze and R. C. Ewing (Elsevier Science Publishers B. V., 1983) p. 427.
20. P. LOISEAU, Ph.D. Thesis, Université Paris VI (France, 2001).
21. G. H. BEALL, *Annu. Rev. Mater. Sci.* **22** (1992) 91.
22. R. GIERE, C. T. WILLIAMS and G. R. LUMPKIN, *Scheiwz. Mineral. Petrog. Mitt.* **78** (1998) 433.
23. P. LOISEAU, D. CAURANT, O. MAJERUS, N. BAFFIER and C. FILLET, *J. Mater. Sci.* **38** (2003).
24. "Phase Diagrams for Ceramists" (Am. Ceram. Soc., 1964) p. 219.
25. R.-G. DUAN, K.-M. LIANG and S. R. GU, *J. Eur. Ceram. Soc.* **18**(2) (1998) 1729.
26. E. Y. VERNAZ and J. L. DUSSOSSOY, *Applied Geochemistry* **1** (1992) 13.
27. T. NOGUCHI and M. MIZUNO, *Bull. Chem. Soc. Jap.* **41**(2) (1968) 2898.
28. H. J. ROSSELL, *J. Solid State Chem.* **99** (1992) 52.
29. D. R. UHLMANN, in "Nucleation and Crystallization in Glasses," vol. 4: Advances in Ceramics, edited by J. H. Simmons, D. R. Uhlmann and G. H. Beall (The Am. Ceram. Soc., 1982) p. 80.
30. G. W. SCHERER and D. R. UHLMANN, *J. Non-Cryst. Solids* **23** (1977) 59.
31. R. J. KIRKPATRICK, L. KLEIN, D. R. UHLMANN and J. H. HAYS, *J. Geophys. Res.* **84**(B7) (1979) 3671.
32. P. F. JAMES, in "Nucleation and Crystallization in Glasses," vol. 4: Advances in Ceramics, edited by J. H. Simmons, D. R. Uhlmann and G. H. Beall (The Am. Ceram. Soc., 1982) p. 1.
33. P. W. MCMILLAN, in "Glass-Ceramics," 2nd edn. (Academic Press, New York, 1979) p. 76.
34. A. RAMOS and M. GANDAIS, *J. Non-Cryst. Solids* **100** (1990) 471.
35. W. VOGEL, in "Glass Chemistry," 2nd edn. (Springer-Verlag, Berlin, 1994) p. 299.
36. E. R. VANCE, C. J. BALL, M. G. BLACKFORD, D. J. CASSIDY and K. L. SMITH, *J. Nucl. Mater.* **175** (1990) 58.

Received 9 August
and accepted 17 October 2002